

Investigating the Hydrogen-Bonding Model of Urea Denaturation

Laura B. Sagle, Yanjie Zhang, Vladislav A. Litosh, Xin Chen, Younhee Cho, and Paul S. Cremer*

Department of Chemistry, Texas A&M University, P.O. Box 30012, College Station, Texas 77843

Received March 2, 2009; E-mail: cremer@mail.chem.tamu.edu

Abstract: The direct binding mechanism for urea-based denaturation of proteins was tested with a thermoresponsive polymer, poly(*N*-isopropylacrylamide) (PNIPAM). Thermodynamic measurements of the polymer's hydrophobic collapse were complemented by Fourier transform infrared (FTIR) spectroscopy, Stokes radius measurements, and methylated urea experiments. It was found that the lower critical solution temperature (LCST) of PNIPAM decreased as urea was added to the solution. Therefore, urea actually facilitated the hydrophobic collapse of the macromolecule. Moreover, these thermodynamic measurements were strongly correlated with amide I band data which indicated that the decrease in the LCST was coupled to the direct hydrogen bonding of urea to the amide moieties of the polymer. In addition, the hydrogen bonding was found to be highly cooperative, which is consistent with a cross-linking (bivalent binding) mechanism. Cross-linking was confirmed by Stokes radius measurements below the polymer's LCST using gel filtration chromatography. Finally, phase transition measurements with methylurea, dimethylurea, and tetramethylurea indicated that these substituted compounds caused the LCST of PNIPAM to rise with increasing methyl group content. No evidence could be found for the direct binding of any of these methylated ureas to the polymer amide moieties by FTIR. These results are inconsistent with a direct hydrogen-bonding mechanism for the urea-induced denaturation of proteins.

Introduction

Although urea was first shown to denature proteins in 1900, the molecular-level mechanism by which this process occurs is not well understood.^{1–5} A central issue concerns whether the mechanism involves direct hydrogen-bonding interactions with biomacromolecules or whether indirect effects via changes in water structure are dominant.^{6–11} Previous studies have shown that urea builds up at the protein–water interface and is capable of hydrogen bonding with both water and amide groups in small molecules.^{12–15} Moreover, urea is known to denature proteins regardless of amino acid composition. Therefore, changes in the solubility of the amide backbone upon the introduction of

urea to solution are considered to be a primary contributor to the denaturation process.^{16–18} If the denaturation mechanism is direct, then hydrogen bonding between urea and the backbone amide groups should be of central importance. However, despite numerous studies, spectroscopic evidence of urea interacting directly with proteins is still largely missing. Such studies would provide critical information as to how hydrogen-bonding interactions relate to relevant thermodynamic parameters.

The absence of spectroscopic data on hydrogen bonding stems from the physiochemical complexity of proteins. Indeed, both infrared and NMR measurements are problematic.^{19,20} For example, analysis of the amide I band in proteins, which predominantly results from the C=O stretch, is a formidable task.^{21,22} Proteins and polypeptides typically show many overlapping peaks in this region that are sensitive to structural changes accompanying urea denaturation.²³ The assignment of these peaks and the distinction of urea binding from structural changes are therefore ambiguous at best. Moreover, proteins consist of amino acids containing many types of side chains, whose absorptions not only can overlap with that of the

- (1) Spiro, K. Z. *Physiol. Chem.* **1900**, 30, 182–199.
- (2) Bennion, B. J.; Daggett, V. *Proc. Natl. Acad. Sci. U.S.A.* **2003**, 100, 5142–5147.
- (3) Auton, M.; Bolen, D. W. *Proc. Natl. Acad. Sci. U.S.A.* **2005**, 102, 15065–15068.
- (4) Hua, L.; Zhou, R. H.; Thirumalai, D.; Berne, B. J. *Proc. Natl. Acad. Sci. U.S.A.* **2008**, 105, 16928–16933.
- (5) Rossky, P. J. *Proc. Natl. Acad. Sci. U.S.A.* **2008**, 105, 16825–16826.
- (6) Pace, N. C.; Tanford, C. *Biochemistry* **1968**, 7, 198–208.
- (7) Robinson, D. R.; Jencks, W. P. *J. Am. Chem. Soc.* **1965**, 87, 2462–2470.
- (8) Frank, H. S.; Franks, F. *J. Chem. Phys.* **1968**, 48, 4746–4757.
- (9) Tobin, D.; Elber, R.; Thirumalai, D. *Biopolymers* **2003**, 68, 359–369.
- (10) Lee, M. E.; van der Vegt, N. F. A. *J. Am. Chem. Soc.* **2006**, 128, 4948–4949.
- (11) Chen, X.; Sagle, L. B.; Cremer, P. S. *J. Am. Chem. Soc.* **2007**, 129, 15104–15106.
- (12) Timasheff, S. N. *Adv. Protein Chem.* **1998**, 51, 355–432.
- (13) Griko, Y. V.; Privalov, P. L. *Biochemistry* **1992**, 31, 8810–8815.
- (14) Triggs, N. E.; Valentini, J. J. *J. Phys. Chem.* **1992**, 96, 6922–6931.
- (15) Pranata, J. *J. Phys. Chem.* **1995**, 99, 4855–4859.

- (16) Auton, M.; Holthausen, L. M. F.; Bolen, D. W. *Proc. Natl. Acad. Sci. U.S.A.* **2007**, 104, 15317–15322.
- (17) Cannon, J. G.; Anderson, C. F.; Record, M. T. *J. Phys. Chem. B* **2007**, 111, 9675–9685.
- (18) Wallqvist, A.; Covell, D. G.; Thirumalai, D. *J. Am. Chem. Soc.* **1998**, 120, 427–428.
- (19) Pastrana-Rios, B. *Biochemistry* **2001**, 40, 9074–9081.
- (20) Dotsch, V.; Wider, G.; Siegal, G.; Wuthrich, K. *FEBS Lett.* **1995**, 366, 6–10.
- (21) Haris, P. I.; Chapman, D. *Biopolymers* **1995**, 37, 251–263.
- (22) Kong, J.; Yu, S. *Acta Biochim. Biophys. Sin.* **2007**, 39, 549–559.
- (23) From, N. B.; Bowler, B. E. *Biochemistry* **1998**, 37, 1623–1631.

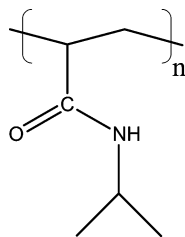


Figure 1. Schematic diagram of poly(*N*-isopropylacrylamide).

backbone but also are capable of interacting with urea.²⁴ To circumvent these problems, we employed a simple polymer model system, PNIPAM, in place of a protein. Such a system should facilitate urea-based denaturation studies by reducing physiochemical complexity and allowing measurements to be made under conditions where spectroscopic signatures are more easily interpreted.

Poly(*N*-isopropylacrylamide) (PNIPAM) is a thermoresponsive polymer which is often used as a simple model for proteins.^{25,26} The structure of this macromolecule is provided in Figure 1. Its molecular weight can be approximately the same as a generic protein, but it possesses a relatively simple chemical structure. Indeed, the only sites for direct interaction of urea with PNIPAM involve the amide moieties. This is because the polymer lacks any other groups capable of accepting or donating a hydrogen bond. Moreover, it is devoid of charged residues, which eliminates the need to consider the interactions of urea with explicit charges. PNIPAM undergoes a lower critical solution temperature (LCST) transition in which collapsed and aggregated structures form upon increasing temperature.²⁷ Such hydrophobic collapse typically involves both intra- and intermolecular hydrogen bonding.^{28,29} This fact has made PNIPAM particularly useful as a mimic for the cold denaturation of proteins.²⁸ Also, the influence of salts on the LCST of this polymer has been shown to follow the Hofmeister series, just as is the case for the physical properties of most proteins.^{30–32}

In stark contrast with proteins, in which the amide I band consists of many overlapping peaks, the amide I band of PNIPAM has been shown to consist of only a single peak near 1625 cm^{−1} when the polymer is fully solvated in aqueous solution.³³ This makes intuitive sense since all the amide moieties are chemically equivalent and have been shown to be hydrogen bonded with water molecules. Upon increasing the solution temperature above PNIPAM's LCST, a second peak appears at ~1652 cm^{−1}, which is similar in frequency to the C=O...H—N hydrogen bonding found in many small-molecule studies.³⁴ This second peak corresponds to the intra- and

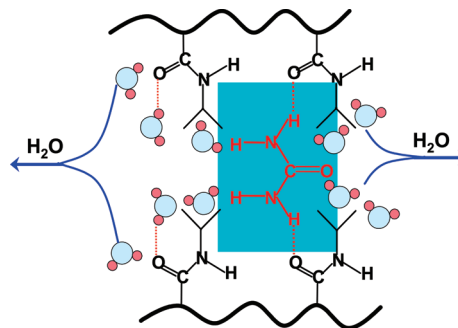


Figure 2. Proposed cross-linking mechanism of PNIPAM by urea.

intermolecular hydrogen bonds formed during hydrophobic collapse and aggregation.³⁵ Due to the lack of secondary and tertiary structure, the peaks that make up the amide I band in PNIPAM can be interpreted simply in terms of bond strengths, making hydrogen-bonding interactions straightforward to assess. In addition, the lack of structure facilitates direct interactions with solution components because the side-chain amide groups are exposed to a greater degree than those in a protein backbone.

In this paper, the hypothesis that urea denatures proteins through direct hydrogen-bonding interactions with amide moieties is explored using amide I band Fourier transform infrared (FTIR) spectroscopy to measure interactions between urea and PNIPAM. To our knowledge, this is the first direct measurement of hydrogen-bonding interactions between urea and a protein-mimetic species. Association isotherms are obtained which show the binding to be highly cooperative and to closely correlate with the decrease of the polymer's LCST. These results are quite striking, as they indicate that hydrogen bonding between urea and PNIPAM actually stabilizes the collapsed rather than the soluble state of the macromolecule. Such a result leads to the idea that urea may interact bivalently with PNIPAM and thereby stabilize its collapse by an intra- and intermolecular cross-linking mechanism (Figure 2). This finding is supported by size exclusion column chromatography measurements which confirm that the Stokes radius of the polymer is decreased as the urea concentration is increased to 5 M, indicating intrachain cross-linking. Beyond this concentration, the apparent radius increases sharply, which is consistent with interchain cross-linking. Finally, studies with monomethylurea, dimethylurea, and tetramethylurea were carried out to limit putative urea cross-linking by hindering hydrogen-bonding interactions. Significantly, these methylated urea analogues showed increasing ability to stabilize the soluble state of PNIPAM with increasing methyl group content. These results undermine the hypothesis that urea denatures proteins via direct hydrogen-bonding interactions with biomacromolecules.

Materials and Methods

Sample Preparation. PNIPAM with a molecular weight of 55 000 g/mol was prepared using methods described previously.^{36,37} Briefly, the polymer was obtained by free radical polymerization of its monomer using *N*-isopropylacrylamide and 2,2'-azobisisobutyronitrile (AIBN) (both from Sigma-Aldrich, St. Louis, MO) as an initiator. Purification of the polymer from the remaining monomer was done by recrystallizing three times using hexanes.

- (24) Barth, A.; Zscherp, C. *Q. Rev. Biophys.* **2002**, *35*, 369–430.
- (25) Schild, H. G.; Tirrell, D. A. *J. Phys. Chem.* **1990**, *94*, 4352–4356.
- (26) Bruscolini, P.; Buzano, C.; Pelizzola, A.; Pretti, M. *Macromol. Symp.* **2002**, *181*, 261–273.
- (27) Schild, H. G. *Prog. Polym. Sci.* **1992**, *17*, 163–249.
- (28) Tiktopulo, E. I.; Uversky, V. N.; Lushchik, V. B.; Klenin, S. I.; Bychkova, V. E.; Ptitsyn, O. B. *Macromolecules* **1995**, *28*, 7519–7524.
- (29) Wang, X. H.; Qiu, X. P.; Wu, C. *Macromolecules* **1998**, *31*, 2972–2976.
- (30) Dhara, D.; Chatterji, P. R. *J. Macromol. Sci.* **2000**, *C40*, 51–68.
- (31) Urry, D. W.; Luan, C. H.; Parker, T. M.; Gowda, D. C.; Prasad, K. U.; Reid, M. C.; Safavy, A. *J. Am. Chem. Soc.* **1991**, *113*, 4346–4348.
- (32) Zhang, Y. J.; Furey, S.; Bergbreiter, D. E.; Cremer, P. S. *J. Am. Chem. Soc.* **2005**, *127*, 14505–14510.
- (33) Maeda, Y.; Higuchi, T.; Ikeda, I. *Langmuir* **2000**, *16*, 7503–7509.
- (34) Herrebout, W. A.; Clou, K.; Desseyn, H. O. *J. Phys. Chem. A* **2001**, *105*, 4865–4881.

- (35) Maeda, Y.; Nakamura, T.; Ikeda, I. *Macromolecules* **2001**, *34*, 1391–1399.
- (36) Fujishige, S. *Polym. J.* **1987**, *19*, 297–300.
- (37) Furey, S.; Zhang, Y. J.; Ortiz-Acosta, D.; Cremer, P. S.; Bergbreiter, D. E. *J. Polym. Sci. A* **2006**, *44*, 1492–1501.

The polydispersity of the PNIPAM solutions was measured using a Viscotek I-MBMMW-3078 mixed-bed column using a Viscotek gel permeation chromatograph. In every case the polydispersity was less than 1.5 with a molecular weight of $\sim 55\,000$ g/mol. These samples were employed in all LCST measurements as well as FTIR studies. PNIPAM samples with a molecular weight of 6400 g/mol were purchased from Polymer Source, Inc. (Quebec, Canada) and used for Stokes radius measurements. These lower molecular weight materials were needed because the Superdex 200 column (Amersham, Piscataway, NJ) used in the gel filtration column chromatography studies required shorter chain lengths for optimal performance.

To make elastin-like polypeptides (ELPs) with 120 pentameric repeats of VPGVG, the corresponding plasmids were expressed in BLR/DE3 *E. coli* cells. In addition to the central 600-residue polypeptide, there were five additional residues on the N-terminus (SKGPG) and two on the C-terminus (WP). The detailed procedures for expressing ELPs have been described previously.³⁸ Purification of the ELPs was carried out with two inverse phase transition cycling steps and verified using sodium dodecyl sulfide–polyacrylamide gel electrophoresis. All ELP and PNIPAM samples were lyophilized and dissolved in urea solutions containing 10 mM sodium phosphate buffer at pH 7.0. Both LCST and FTIR measurements were carried out at PNIPAM and ELP concentrations of 10 mg/mL and 6 mg/mL, respectively.

For vibrational studies of the amide I band, it was necessary to employ ^{13}C -labeled urea (Cambridge Isotopes Inc., Andover, MA), as this isotope red-shifted the carbonyl absorption of the osmolyte by $\sim 60\text{ cm}^{-1}$.³⁹ This was done to remove this peak from the amide I band region at $\sim 1625\text{ cm}^{-1}$. Isotopically labeled methylurea and dimethylurea were also required for the same purpose, but these compounds were not commercially available. They were therefore synthesized using standard procedures.⁴⁰ To make the isotopically labeled compounds, ^{13}C -labeled urea (12.2 g, 0.2 mol) was mixed with methylamine hydrochloride (Sigma-Aldrich) (27.0 g, 0.4 mol) and heated to 160–70 °C for 1 h under a nitrogen atmosphere. The resulting cake was cooled to room temperature, suspended in dichloromethane, and subjected to column chromatography (0–5% methanol in dichloromethane), which produced the separated 1,3-dimethylurea- ^{13}C and methylurea- ^{13}C species in yields of 57% and 39%, respectively. The first compound removed from the column and tested by NMR was 1,3-dimethylurea- ^{13}C (10.2 g, 57%): ^1H NMR (400 MHz, DMSO- d_6) δ 5.72 (br s, 2 H, D_2O exchangeable, NH), 2.52 (t, $J = 4.0$ Hz, 6 H). Next, methylurea- ^{13}C was removed from the column and tested by NMR (5.8 g, 39%): ^1H NMR (400 MHz, DMSO- d_6) δ 5.77 (br s, 1 H, D_2O exchangeable, NH), 5.40 (br s, 2 H), 2.50 (d, $J = 4.0$ Hz).

LCST Measurements. LCST measurements were carried out using a microfluidic temperature gradient apparatus described previously.^{41,42} Briefly, a cover glass was placed on top of two parallel brass tubes (1/8 in. wide, K&S Engineering, Chicago, IL) through which hot and cold antifreeze solutions were flowed using bath circulators (Fisher Scientific, Pittsburgh, PA). Rectangular borosilicate capillary tubes (VitroCom, Inc., Mountain Lakes, NJ) with dimensions of 2 cm \times 1 mm \times 100 μm (length \times width \times height) were used as sample containers and placed perpendicular to the brass tubes. Light scattering from the samples was monitored with a CCD camera (Micromax 1024, Princeton Instruments, Trenton, NJ) using dark-field optics under an inverted microscope (TE2000-U, Nikon). Two different polymer solutions with previously measured LCSTs served to calibrate the slope of the

temperature gradient for each experiment. The temperature along the capillary tubes was determined by counting the pixels in a linescan drawn along the temperature gradient in the CCD images.

Amide I Band ATR-FTIR Measurements. Fourier transform infrared spectra were taken with a Nicolet 470 FTIR spectrometer equipped with a liquid nitrogen cooled MCT detector (Thermo Electron Corp., Madison, WI) and a Pike Miracle attenuated total reflection (ATR) setup containing a single-bounce ZnSe crystal (Pike Technologies, Madison WI). The settings used during data acquisition were as follows: 256 scans, one level of zero-filling, and the Blackman–Harris apodization function. Background spectra were taken directly before sample spectra and subtracted from the latter. Specifically, for each sample containing PNIPAM, an otherwise identical urea solution without the polymer was used as the control. In all cases it was found that the subtraction factor for the contribution of buffer and urea to the vibrational spectrum was very close to unity. Furthermore, baseline correction was carried out in Matlab (Student Version 6.5, equipped with curve-fitting and optimization toolboxes, Mathworks, Natick, MA) by subtracting polynomials in order to make the baseline flat around the peaks of interest. Spectral fitting was also carried out in Matlab with peak frequencies restricted to a 6 cm^{-1} window and linewidths restricted to an upper limit of 100 cm^{-1} . The quality of the spectral fits was judged by the least error sum method, and all spectral fits shown have the lowest least error sum. The number of Gaussians required to fit a given spectrum was determined using a second derivative test and a statistical *F*-test analysis at the 99% confidence limit.⁴³

Gel Filtration Column Chromatography. Gel filtration column chromatography for Stokes radius measurements was carried out using an AKTA FPLC system equipped with a UPC-900 monitor, an M-925 mixing chamber, and a P-920 pump (Amersham, Piscataway, NJ). The Superdex 200 column was equilibrated in the appropriate urea solution by running an amount of liquid through it that was at least three times the column volume. Samples were dissolved in the same solution used to equilibrate the column, and 1 mL of sample (10 mg/mL) was loaded using a 2 mL sample loop. The column was equilibrated, and samples were run at 4 °C to ensure the polymer remained in the uncollapsed state. Aliquots were collected every minute after loading the polymer samples. These eluted solutions were heated to 70 °C and visually inspected for cloudiness.

The Stokes radius is proportional to a partition coefficient ($1/K_d$) which is calculated from the elution volumes of the sample and two standards.⁴⁴ For this purpose, solutions of blue dextran (1 mL of 0.5 mg/mL) and 3'-cytidine monophosphate (3'CMP, 1 mL of 0.002 mg/mL) were also dissolved in the same urea solutions that were used with PNIPAM. These two standards, as well as the PNIPAM samples, were injected and eluted in separate runs. The partition coefficient, K_d (which is inversely proportional to the Stokes radius), was calculated according to the following equation:

$$K_d = (V_{e\text{PN}} - V_{e\text{BD}})/(V_{e\text{3'CMP}} - V_{e\text{BD}}) \quad (1)$$

where $V_{e\text{PN}}$, $V_{e\text{BD}}$, and $V_{e\text{3'CMP}}$ are the volumes of the PNIPAM sample, blue dextran, and 3'CMP, respectively. The ratio of the Stokes radius in urea versus water was calculated from $[1/K_d(\text{in urea})]/[1/K_d(\text{in water})]$.⁴⁵ It should be noted that the elution volume was determined as the time it took for elution of the first cloudy sample multiplied by the flow rate of the solution through the column.

Results

LCST Values for PNIPAM and ELP vs Urea Concentration. LCST values for PNIPAM were measured in 10 mM phosphate buffer at pH 7.0 with increasing concentrations of urea (Figure

(38) Meyer, D. E.; Chilkoti, A. *Biomacromolecules* **2002**, *3*, 357–367.

(39) Fabian, H.; Mantsch, H. H. *Biochemistry* **1995**, *34*, 13651–13655.

(40) Davis, T. L.; Blanchard, K. C. *J. Am. Chem. Soc.* **1923**, *45*, 1816–1820.

(41) Mao, H. B.; Li, C. M.; Zhang, Y. J.; Bergbreiter, D. E.; Cremer, P. S. *J. Am. Chem. Soc.* **2003**, *125*, 2850–2851.

(42) Zhang, Y. J.; Mao, H. B.; Cremer, P. S. *Biophys. J.* **2003**, *84*, 502a–503a.

(43) Snedecor, G. W.; Cochran, W. G. *Statistical Methods*, 8th ed.; Iowa State University Press: Ames, IA, 1989.

(44) Baskakov, I. V.; Bolen, D. W. *Biochemistry* **1998**, *37*, 18010–18017.

(45) Qu, Y. X.; Bolen, C. L.; Bolen, D. W. *Proc. Natl. Acad. Sci. U.S.A.* **1998**, *95*, 9268–9273.

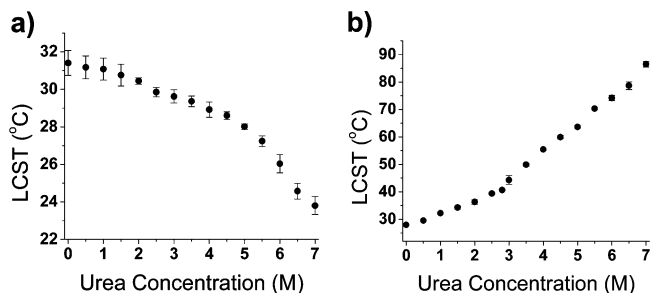


Figure 3. LCST trends for (a) PNIPAM and (b) ELP with increasing urea concentration.

3a). As a control, LCST measurements were also run with an ELP under the same conditions (Figure 3b). The ELP consisted of 120 pentameric repeats of Val-Pro-Gly-Val-Gly (600 residues total). Like PNIPAM, it is a thermoresponsive polymer that undergoes an inverse phase transition upon heating. With the exception of the two ends, this biopolymer contains no charged residues or side chains capable of undergoing hydrogen bonding with urea. Therefore, it should predominantly interact with urea through its backbone amide moieties.

The dramatic increase in the LCST of the ELP with increasing urea concentration reflects the improved stability of the uncollapsed, soluble state of the polypeptide. This is the same behavior that is observed with the vast majority of proteins.^{46,47} In stark contrast to this result, PNIPAM shows the opposite trend. Namely, urea stabilizes the collapsed and aggregated state of the polymer. Studies with proteins have shown that a cross-linking agent, such as glutaraldehyde, or disulfide bond formation greatly increases the stability of the collapsed or molten globule state of a protein.^{48,49} By analogy, the NH_2 groups of urea may interact with the amide groups of PNIPAM in a bivalent manner, which in turn could bring the chains into closer proximity with one another, thereby stabilizing the collapsed state (Figure 2). This hypothesis is explored in the experiments described below.

Amide I Band ATR/FTIR Measurements with Urea and PNIPAM. To investigate hydrogen-bonding interactions between urea and PNIPAM, amide I band ATR/FTIR spectroscopy was carried out. In a first set of measurements, the FTIR spectrum of PNIPAM was measured in an aqueous solution at 10 °C (Figure 4a). Since this is well below the LCST, the polymer was fully soluble in water. As can be seen from the data, the amide I band consisted of a single peak at $\sim 1625\text{ cm}^{-1}$. This indicates that all the carbonyl groups are hydrogen bonded to water.⁵⁰ A second peak arose at 1560 cm^{-1} , which is associated with the amide II band and will not be discussed further. Upon raising the temperature above the LCST (40 °C), a third peak appeared at $\sim 1652\text{ cm}^{-1}$ (Figure 4b). As noted in the Introduction, this higher frequency feature is known to be indicative of $\text{C}=\text{O}\cdots\text{H}-\text{N}$ hydrogen bonding.³³ Such a result is expected because intra- and intermolecular hydrogen bonding should occur concomitantly with the hydrophobic collapse of PNIPAM. Next, experiments were performed below the LCST (10 °C)

with 6 M ^{13}C -labeled urea. As can be seen, a high-frequency peak appears at the same position as in the collapsed form of the polymer (Figure 4c). Since the measurements were carried out below the phase transition temperature, the higher frequency peak in Figure 4c should not be due to intra- or intermolecular hydrogen bonding.

To aid in the assignment of the 1652 cm^{-1} peak for the uncollapsed polymer, measurements were carried out in D_2O instead of H_2O with PNIPAM at 10 °C while still using ^{13}C -labeled urea. As expected, the peak was red-shifted to $\sim 1646\text{ cm}^{-1}$, which is consistent with $\text{C}=\text{O}\cdots\text{D}-\text{N}$ formation.³⁵ In order to further confirm the assignment of this peak, spectra were collected in 6 M ^{13}C , ^{15}N -labeled urea in H_2O . In this case, the frequency of the amide I band red-shifted by $\sim 2.5\text{ cm}^{-1}$, which is consistent with $\text{C}=\text{O}\cdots\text{H}-^{15}\text{N}$ bonding.⁵¹ The high-frequency peak in the amide I band spectrum of PNIPAM can therefore be assigned to $\text{C}=\text{O}\cdots\text{H}-\text{N}$ for the hydrogen bonding of PNIPAM with urea as depicted in the schematic diagram associated with Figure 4c. The spectra with ^{15}N -labeled urea and heavy water are provided in the Supporting Information. Spectra corresponding to many other urea concentrations in D_2O and H_2O are also provided in the Supporting Information. It was found that the high-frequency feature grew continuously as the urea concentration was varied from 0 to 6.5 M.

Next, the fraction of urea bound to PNIPAM was determined directly from the vibrational spectroscopy data. This could be done by calculating the area of the 1652 cm^{-1} peak and dividing its value by the sum of the areas of the 1625 and 1652 cm^{-1} peaks (Figure 5a, black squares). As can be seen, the bound fraction of urea does not vary linearly with concentration. In fact, the bound fraction increases more rapidly above 4 M. This type of concentration dependence is expected from a cooperative binding process, which is in turn consistent with a cross-linking mechanism. Indeed, initial bivalent urea binding should bring the PNIPAM chains closer together, which would induce additional urea molecules to bind to the proximal chains. As noted above, these data were only taken up to 6.5 M urea. As a consequence, the leveling-off of what is presumably a sigmoidal curve shape was not completed. The reason data were not acquired at higher osmolyte concentrations was the interference of the carbonyl stretch from the isotopically labeled urea with the amide I band peaks. Once the urea peak became sufficiently large, the spectral quality was significantly reduced, and it was difficult to reliably perform a spectral subtraction and properly fit the amide peaks.

Also plotted in Figure 5a is the decrease in the LCST value induced by the addition of urea (red circles). These values were calculated from the data in Figure 3b by subtracting the value of the LCST in the presence of urea at each concentration from the value of the LCST in its absence. As can be seen, there was a strong correlation between the fraction of urea bound (as measured by FTIR spectroscopy) and the fall in the LCST value. Thus, it appears that the hydrogen bonding of urea with PNIPAM is directly coupled with the observed changes in the phase transition temperature. A set of experiments identical to those shown in Figure 5a, but taken with D_2O , is shown in Figure 5b. The relationship between the LCST and the fraction of urea bound was the same in that case. Again, the relationship between the fraction of urea bound to PNIPAM and the bulk concentration of this osmolyte was nonlinear.

(46) Schellman, J. A. *Biophys. Chem.* **2002**, *96*, 91–101.

(47) Pace, C. N.; Marshall, H. F. *Arch. Biochem. Biophys.* **1980**, *199*, 270–276.

(48) Pace, C. N.; Grimsley, G. R.; Thomson, J. A.; Barnett, B. J. *J. Biol. Chem.* **1988**, *263*, 11820–11825.

(49) *Prediction of Protein Structure and the Principles of Protein Conformation*; Fasman, G. D., Ed.; Plenum Press: New York, 1989; p 161.

(50) Yamauchi, H.; Maeda, Y. *J. Phys. Chem. B* **2007**, *111*, 12964–12968.

(51) Tanimoto, T.; Shibata, M.; Belenky, M.; Herzfeld, J.; Kandori, H. *Biochemistry* **2004**, *43*, 9439–9447.

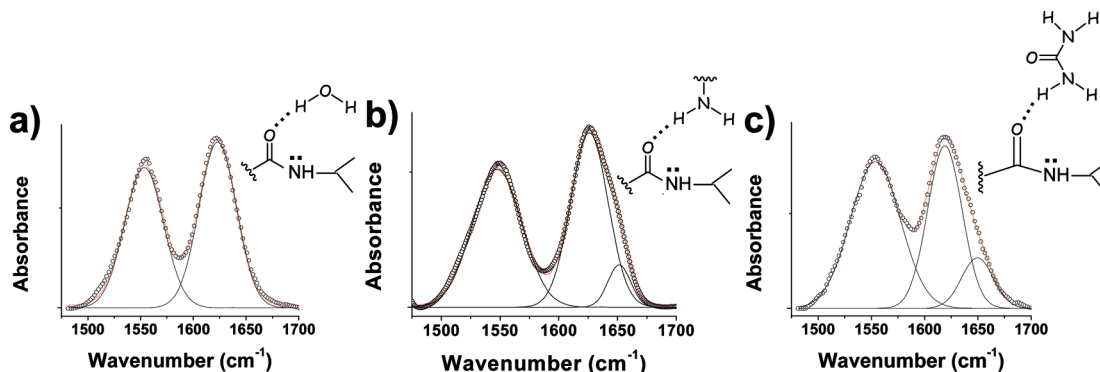


Figure 4. FTIR spectra of the amide I and II bands for PNIPAM at (a) 10 °C, (b) 40 °C, and (c) 10 °C in the presence of 6 M ^{13}C -labeled urea. A schematic diagram showing the type of hydrogen bonding involved in each spectrum is also shown.

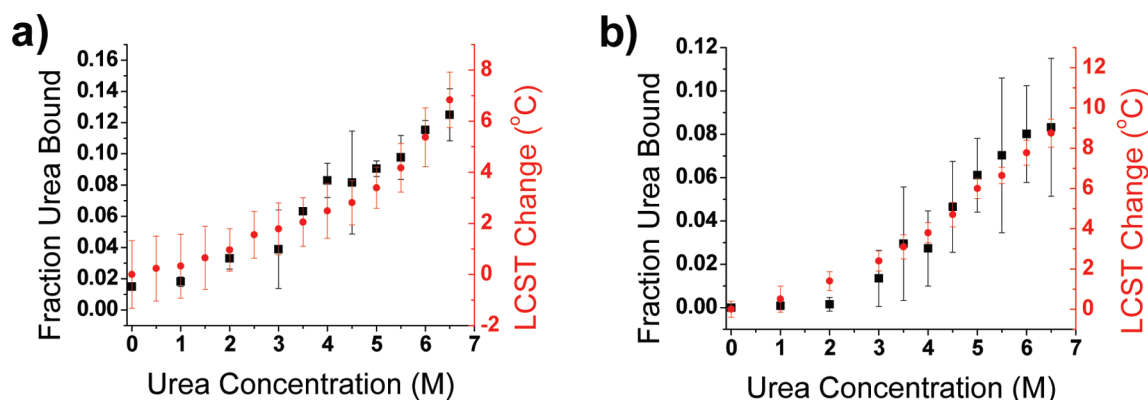


Figure 5. Curves showing the fraction of urea bound to PNIPAM with increasing urea concentration (black squares) in (a) H_2O and (b) D_2O . Also shown (red circles) is the change in LCST (LCST in 0 M urea minus the LCST at a given urea concentration) in (a) H_2O and (b) D_2O .

It should be noted that amide I band measurements were also carried with varying urea concentrations with the ELP (see Supporting Information). However, due to the presence of secondary structure, the amide I band consisted of at least three overlapping peaks which also overlapped with the putative position of the peak from hydrogen-bonded urea. This made it impossible to discern whether hydrogen bonding between the polypeptide and the osmolyte was occurring with any degree of certainty.

Gel Filtration Column Chromatography Studies. Stokes radius measurements were carried out at 10 °C using gel filtration column chromatography to test the idea that urea cross-linked the chains of PNIPAM together. The radii of the polymer aggregates were determined according to eq 1. Figure 6 shows a plot of the Stokes radius of PNIPAM as a function of the urea concentration. Specifically, the y-axis plots the Stokes radius in urea solution normalized to the value in a phosphate buffer solution. As can be seen, this ratio decreased until about 5 M, where it reached a minimum. At that point, the value rose sharply. The low-concentration results were consistent with the notion that bivalent urea binding cross-linked the PNIPAM chains, which decreased the Stokes radius of the polymer and induced hydrophobic collapse. At sufficient urea concentration, however, intermolecular cross-linking became dominant, and the increasing size of the polymer aggregates led to larger Stokes radius values.

Altering Urea's Ability To Hydrogen-Bond to PNIPAM. In a final set of experiments, substituted urea compounds were employed to determine if these molecules could reverse the thermodynamic trends observed in Figure 2. Since urea interacts

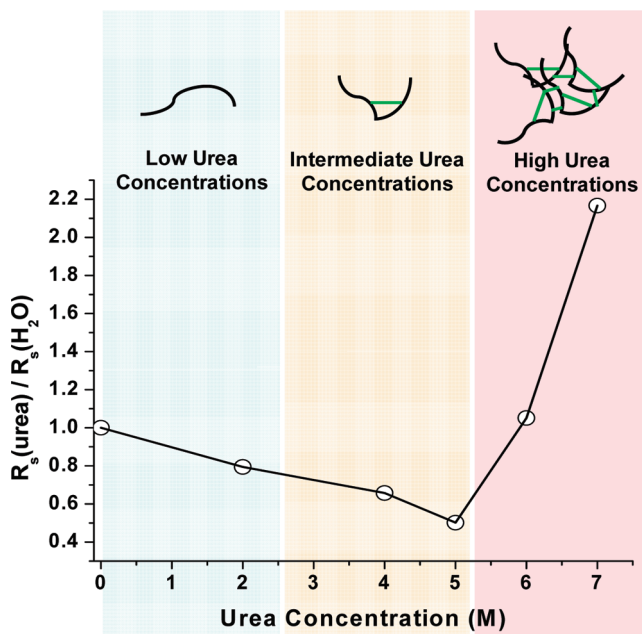


Figure 6. Stokes radii measurements of PNIPAM as a function of urea concentration by gel filtration column chromatography. All measurements were carried out at 10 °C. The lines drawn between the points are a guide to the eye.

with PNIPAM through its NH_2 groups, attaching methyl substituents to the nitrogen atoms should provide steric hindrance to hydrogen bonding. Indeed, monomethylurea should

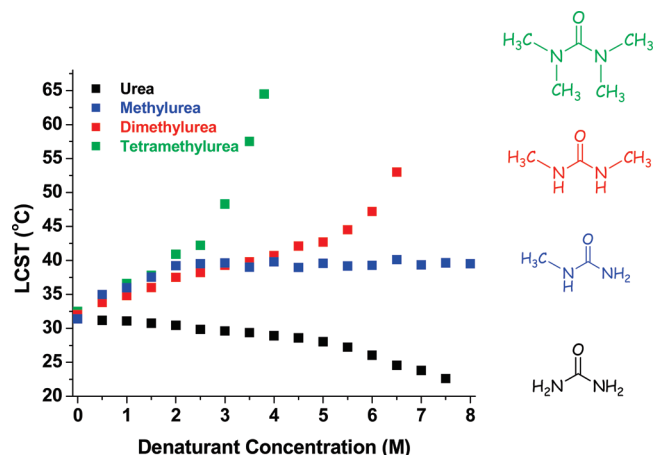


Figure 7. LCST trends for PNIPAM as a function of osmolyte concentration. The results for each osmolyte are color coded.

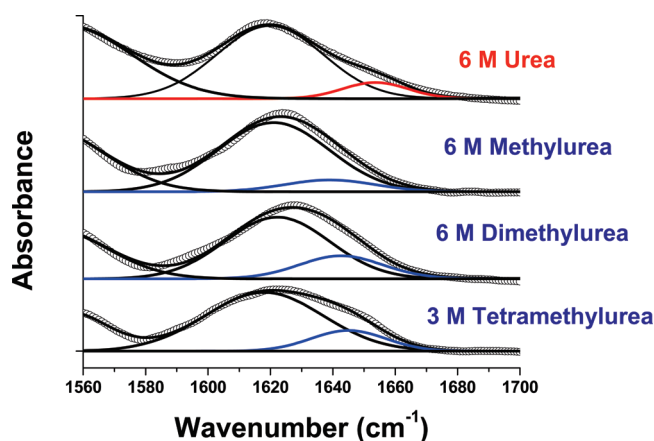


Figure 8. Amide I band ATR-FTIR spectra for urea, methylurea, dimethylurea, and tetramethylurea. The overall fits to the data are shown as solid lines, while the individual data points are shown as circles. The fits for the individual high-frequency peaks for the methyl-terminated ureas are provided in blue ($\sim 1644\text{ cm}^{-1}$), while the same peak with urea is shown in red ($\sim 1652\text{ cm}^{-1}$).

strongly inhibit urea's cross-linking ability. Dimethylurea should be able to prevent binding to an even larger extent, and tetramethylurea should be able to entirely inhibit such bonding. The LCST values vs osmolyte concentrations for these substituted ureas are plotted in Figure 7. As can be seen, the methylated ureas did indeed prevent the collapse of PNIPAM. Specifically, the addition of monomethylurea slightly favored the uncollapsed state of the polymer. The thermodynamic effects of dimethylurea and tetramethylurea were even more dramatic. These results were strong additional support for the notion that the direct binding of urea led to cross-linking and the stabilization of the collapsed state.

Amide I band FTIR measurements were carried out with PNIPAM in the presence of ^{13}C -labeled monomethylurea, dimethylurea, and tetramethylurea, respectively, to gain molecular-level insight into the interactions between the substituted ureas and the thermoresponsive polymer. These results are shown in Figure 8. Similar to the observation with urea, the presence of methylated ureas also gave rise to a high-frequency peak that appeared with increasing osmolyte concentration. In these cases, however, the frequency of this peak was different than that found with urea. Specifically, the feature was centered at 1644 cm^{-1} instead of 1652 cm^{-1} . The fact that the identical

peak was present even with tetramethylurea, which has no available NH groups, was strong evidence that it was not caused by hydrogen bonding between the osmolytes and the polymer. Of course, methylated ureas could hydrogen bond through their C=O groups instead of the NH groups. However, it is well documented in the literature that hydrogen bonding to amide groups in this fashion would lead to enol stabilization, which leads to a red shift from the 1625 cm^{-1} position, not a blue shift as observed.^{52–54} Thus, the methylated ureas did not appear to be directly interacting with PNIPAM through hydrogen-bonding interactions. Therefore, this peak likely arises from an altered interaction between the polymer and adjacent water molecules, as will be discussed below.

Discussion

Thermodynamics and Bivalency. As noted in the Introduction, it is extremely difficult to determine the extent of hydrogen bonding between a protein and urea by employing FTIR or NMR measurements. In previous studies, estimates of urea binding to proteins have been inferred from calorimetry and transfer free energy data.^{55,56} If the mechanism for urea-induced protein denaturation does not involve direct hydrogen bonding, then it is not necessarily the case that such estimates are valid. Nevertheless, indirect measurements have typically produced apparent K_d values ranging from 3.4 to 12.5 M. Additionally, a recent study using end-to-end diffusion rates and invoking the Schellman weak binding model yielded an apparent K_d value of 3.8 M.⁵⁷ It should be noted that the Schellman model of statistical interactions between urea and proteins does not account for cooperative or bivalent binding.⁵⁸

We have directly measured the fraction of urea bound to PNIPAM as a function of urea concentration (Figure 5). The FTIR measurements exhibited small intensity values for the 1652 cm^{-1} peak below 3 M urea (Figure 4 and Supporting Information). This peak, however, rose sharply above this value. Such a result was consistent with a cooperative or bivalent binding mechanism. Specifically, the vibrational data were consistent with the NH of urea hydrogen-bonding to the carbonyl moieties of the polymer (Figure 2). This mechanism was supported by the substituted urea studies, which showed that even a single methyl group was sufficient to remove any evidence for the 1652 cm^{-1} feature for up to 6 M methylurea (Figure 8). Moreover, Stokes radius measurements (Figure 6) were also consistent with a cross-linking mechanism. Since the binding curves did not level off by 6.5 M urea, it was not possible to abstract a K_d value from these data. Nevertheless, a lower bound for this number would be greater than 5 M based upon the trend in Figure 5.

It is expected that hydrogen bonding between urea and polypeptides should be weaker than the corresponding PNIPAM–urea bonding. This is because the urea-induced hydrophobic collapse of PNIPAM is highly cooperative (Figure 5). Moreover, the amide moieties in PNIPAM are relatively more available to urea binding because they are pendant groups as opposed to polypeptide amides that are part of the backbone. In addition,

(52) Ramondo, F.; Cesaro, S. N.; Bencivenni, L. *J. Mol. Struct.* **1993**, 291, 219–244.

(53) Dudek, G. O. *J. Org. Chem.* **1965**, 30, 548–552.

(54) Dudek, G. O.; Volpp, G. P. *J. Org. Chem.* **1965**, 30, 50–54.

(55) Pace, C. N. *Methods Enzymol.* **1986**, 131, 266–280.

(56) Makhatadze, G. I.; Privalov, P. L. *J. Mol. Biol.* **1992**, 226, 491–505.

(57) Moglich, A.; Krieger, F.; Kiefhaber, T. *J. Mol. Biol.* **2005**, 345, 153–162.

(58) Schellman, J. A. *Biopolymers* **1987**, 26, 549–559.

interactions between monomethylurea and PNIPAM were not observed, which is strong evidence that monovalent interactions are significantly weaker than their bivalent counterparts. By extension, monovalent interactions between peptides and urea would also be expected to be very weak. It should be noted that bivalent interactions between urea and polypeptides can be excluded in most cases because these interactions should stabilize the collapsed state of proteins in analogy to the results from PNIPAM. Therefore, one would expect that the equilibrium dissociation constant for urea binding to proteins should be much larger than 5 M.

Significantly, there is a direct correlation between the hydrogen bonding of urea and the observed LCST trend for PNIPAM. Thus, hydrogen bonding of urea to this polymer appears to be responsible for the stabilization of the collapsed state. However, this thermodynamic stabilization is relatively modest, $\sim 7^\circ\text{C}$ in 6.5 M urea. Therefore, since the binding of urea to a polypeptide is expected to be even weaker than that to PNIPAM, it would be very difficult to account for the large and general denaturing effects observed with proteins on the basis of direct binding interactions alone.

Methylated Urea Molecules and the 1644 cm^{-1} Feature. The LCST of PNIPAM at fixed osmolyte concentration increased with increasing urea methylation (Figure 7). Specifically, tetramethylurea was particularly effective at increasing PNIPAM's LCST. This behavior is consistent with that of proteins, for which osmolyte denaturation efficacy has also been shown to increase with the increasing number of methyl substituent groups.⁴⁷ Since tetramethylurea has no NH moieties, the mechanism by which it raises the LCST cannot involve the formation of hydrogen bonds with the carbonyl moieties of PNIPAM. Therefore, the presence of the broad absorption feature centered near 1644 cm^{-1} for all three methylated urea compounds in Figure 8 was quite curious.

In principle, the 1644 cm^{-1} absorption feature might be caused by a change in the local dielectric constant due to neighboring solute molecules or geometric effects.^{59,60} However, all the methylated ureas gave rise to the same feature at the identical frequency while not affecting the frequency of the larger band at 1625 cm^{-1} . As such, this possibility is deemed to be rather unlikely. Instead, we postulate that this high-frequency amide I peak was caused by changes in the hydrogen bonding of the thermoresponsive polymer with adjacent water molecules. Recent studies have shown that water molecules in the vicinity of hydrophobic solutes such as tetramethylurea were perturbed due to steric effects.^{61,62} These water molecules have a weakened hydrogen-bonding network in which the hydrogen bonds themselves are similar to those of bulk water but the coordination number is lower. Since denaturants like tetramethylurea are known to build up at the protein–water interface,⁶³ it is at least plausible that urea-based osmolytes lower the number of water molecules that can coordinate with the $\text{C}=\text{O}$ groups of the polymer, which may in turn cause the observed 1644 cm^{-1} peak.

Nonspecific Urea Hypothesis. An abundance of literature data supports the notion that denaturants such as dimethyl- and tetramethylurea unfold proteins through an indirect, hydrophobic mechanism. Transfer and viscosity data of hydrophobic solutes in the presence of methylated ureas have shown an increase in solubility with increasing methyl group content on the osmolyte.^{64,65} In addition, NMR,⁶⁶ dielectric relaxation,⁶⁷ and femtosecond mid-infrared spectroscopy⁶⁸ studies all indicated changes in water structure upon addition of methylated urea molecules. If the mechanism for urea denaturation of proteins is analogous to that of its methyl-substituted analogues, then the reasons why urea is a less powerful denaturant are clear. The increasing of denaturing abilities with increasing methyl substitution closely matches their ability to decrease the surface tension of an air–water interface.⁶⁹ Since more substituted ureas more effectively build up at hydrophobic interfaces, their effective interfacial concentrations are higher. By contrast with the methyl-substituted analogues, urea actually raises the surface tension of the air–water interface. Therefore, larger bulk concentrations would be needed to achieve similar interfacial concentrations.

The molecular-level basis for urea denaturation of proteins certainly should involve the solvation of the amide backbone.^{17,70} However, instead of being based on hydrogen bonding, the mechanism may involve the displacement of water by the larger osmolyte molecules based on entropic considerations.⁷¹ Moreover, urea may affect interfacial water structure in a manner that leads to increased solubility of the amide and hydrophobic portions of proteins compared with an aqueous solution.⁷² Finally, the interactions between denaturant molecules and hydrophobic side chains may also need to be considered.⁷³

Acknowledgment. This work was supported by the National Science Foundation (CHE-0809854) and the Welch Foundation (A-1421) to P.S.C. We thank Prof. Ashutosh Chilkoti and Dr. Kimberly Trabbic-Carlson for kindly supplying the ELP plasmids used in this study. In addition, we thank Prof. David Bergbreiter and Steven Furyk for synthesizing 55 000 g/mol PNIPAM.

Supporting Information Available: Detailed experimental procedures for all the measurements carried out as well as FTIR data in H_2O and D_2O and with ^{13}C , ^{15}N -labeled urea. This material is available free of charge via the Internet at <http://pubs.acs.org>.

JA9016057

- (59) Katsumoto, Y.; Tanaka, T.; Ozaki, Y. *J. Phys. Chem. B* **2005**, *109*, 20690–20696.
(60) Viswanathan, R.; Dannenberg, J. J. *J. Phys. Chem. B* **2008**, *112*, 5199–5208.
(61) Rezus, Y. L. A.; Bakker, H. J. *Phys. Rev. Lett.* **2007**, *99*, 148301.
(62) Gallagher, K. R.; Sharp, K. A. *J. Am. Chem. Soc.* **2003**, *125*, 9853–9860.
(63) Gordon, J. A. *Biochemistry* **1972**, *11*, 1862–1870.

- (64) Tanford, C. *Adv. Protein Chem.* **1970**, *24*, 1–95.
(65) Singh, M.; Kumar, A. *J. Solution Chem.* **2006**, *35*, 567–582.
(66) Haselmeier, R.; Holz, M.; Marbach, W.; Weingartner, H. *J. Phys. Chem.* **1995**, *99*, 2243–2246.
(67) Kaatz, U.; Gerke, H.; Pottel, R. *J. Phys. Chem.* **1986**, *90*, 5464–5469.
(68) Rezus, Y. L. A.; Bakker, H. J. *J. Phys. Chem. A* **2008**, *112*, 2355–2361.
(69) The data for surface tension measurements were taken with a CAM 200 optical contact angle meter (KSV Instruments, Monroe, CT).
(70) Street, T. O.; Bolen, D. W.; Rose, G. D. *Proc. Natl. Acad. Sci. U.S.A.* **2006**, *103*, 13997–14002.
(71) Kuharski, R. A.; Rossky, P. J. *J. Am. Chem. Soc.* **1984**, *106*, 5794–5800.
(72) Granick, S.; Bae, S. C. *Science* **2008**, *322*, 1477–1478.
(73) Zangi, R.; Zhou, R. H.; Berne, B. J. *J. Am. Chem. Soc.* **2009**, *131*, 1535–1541.